# Inactivation of the Potassium Conductance and Related Phenomena Caused by Quaternary Ammonium Ion Injection in Squid Axons

CLAY M. ARMSTRONG

From the Departments of Physiology and Neurology, Duke University Medical Center, Durham, North Carolina 27706, and Laboratorio de Fisiología Celular, Montemar, Chile. Dr. Armstrong's present address is Department of Physiology, University of Rochester School of Medicine and Dentistry, Rochester, New York 14620

ABSTRACT    Several analogues of the tetraethylammonium (TEA$^+$) ion were injected into the giant axon of the squid, and the resultant changes in time course and magnitude of the potassium current ($I_K$) were studied. For all the analogues used, three of the ethyl side chains of TEA$^+$ were left unchanged, while the fourth chain was either lengthened or shortened. Increasing the length of this chain increased binding to the blocking site in the channel by a factor of roughly two for each added $CH_2$ group. The effect on the rate of entry into the blocking site was relatively slight. Thus the concentration for half-suppression of $g_K$ decreased by about the same factor of two for each added $CH_2$. All the analogues caused anomalous or ingoing rectification. The longest chain analogue used, pentyltriethylammonium ion, caused rapid inactivation of $g_K$, and this inactivation had properties quite similar to $g_{Na}$ inactivation. The anomalous rectification and the $g_K$ inactivation caused by these compounds have the same basic mechanism.

## INTRODUCTION

The tetraethylammonium ion (TEA$^+$) is known to have a number of effects on the potassium permeability of nerve membranes that are of considerable interest. It prolongs the action potential of nerve fibers by selectively eliminating potassium permeability (Hagiwara and Saito, 1959; Armstrong and Binstock, 1965; Schmidt and Stämpfli, 1966; Nakajima, 1966; Koppenhöfer, 1967; Hille, 1967 b). When injected into a squid axon it causes anomalous or ingoing rectification of the potassium current (Armstrong and Binstock, 1965), a type of rectification seen in muscle fibers (Katz, 1949; Noble, 1962; Nakajima et al., 1962) but never in a normal squid nerve fiber. At low axoplasmic concentrations it produces changes in the voltage clamp currents from which it is possible to estimate the density of potassium channels in the membrane,

553

yielding a figure of 67 channels/$\mu^2$ (Armstrong, 1966 b). For the squid axon all the effects of TEA$^+$ can be accounted for qualitatively by saying that it binds to blocking sites in the potassium channels that are accessible only from the inside, and only when the voltage-sensitive gates that normally control potassium permeability (Hodgkin and Huxley, 1952 b) are open; and that inward current through the channels sweeps them clear of the blocking ions.

What features of the TEA$^+$ ion enable it to enter the K$^+$ channel, and why does it stick there after entering? Speculations on these matters published elsewhere (Armstrong, 1966 a) are: TEA$^+$ can enter the channel because its radius is the same as that of a K$^+$ ion with one hydration shell; and that sticking is a result of electrostatic bonding to a site in the channel. These matters are amenable to investigation by altering the TEA$^+$ molecule; i.e., by using analogues of TEA$^+$. A large number of quaternary ammonium ions more or less similar to TEA$^+$ were applied to the frog node by Hille (1967 a) who found that all the compounds which he used were less effective than TEA$^+$ in lowering $g_K$. For investigations of this type, the frog node is a less favorable preparation than the squid axon because one does not see current transients indicative of movements of the blocking ion. For this reason it is possible to determine only the ratio of the rate constants of entering and leaving the channels or blocking sites, and not the individual constants. In the squid axon, on the other hand, it is possible to determine the individual constants. This paper reports on the changes in these rate constants produced by simple alterations of the TEA$^+$ ion: three of the ethyl groups were left unchanged, while the fourth side chain was either lengthened or shortened. All the compounds tested cause anomalous or ingoing rectification. The major new finding is that adding —CH$_2$ groups to the fourth chain enhances binding to the blocking site. One result is that fibers containing long chain analogues display a rapid inactivation of $g_K$ that resembles $g_{Na}$ inactivation (Hodgkin and Huxley, 1952 a). This rapid $g_K$ inactivation is altogether distinct from the slow inactivation seen in squid (Ehrenstein and Gilbert, 1966) and in muscle (Nakajima et al., 1962; Adrian et al., 1968). On the other hand it is quite similar to the $g_K$ inactivation described by Nakajima and Kusano (1966) in puffer fish neurons. It is shown here that rapid $g_K$ inactivation (hereafter called simply inactivation) and anomalous rectification, both of which are induced in squid axons by quaternary ammonium ions, share the same basic mechanism.

## METHODS

These experiments were performed on the Chilean squid, *Dosidicus gigas*, using, in general, techniques described previously. The voltage clamp circuit was a somewhat modified version of the one given in Armstrong and Binstock (1964). Because of the large diameter of the axons, coaxial potential and current electrodes were found unnecessary. Instead, platinum wire, 100 $\mu$ in diameter, platinized for a length of

32 mm, was introduced from one end of the axon to supply current; and a pipette, about 100 $\mu$ outside diameter, filled with M/2 KCl, and with an electrically floating platinum wire through the narrow part, was introduced from the other end to measure membrane potential $(V_m)$. The resistance in series with the membrane $(R_s)$ was determined by measuring $V_m$ changes caused by brief current steps (Fig. 1 a). $R_s$, which is proportional to the initial step in the record (arrow), was usually about 8 ohm cm². After determining the membrane area (see below), this resistance was compensated for as described previously (Armstrong and Binstock, 1964). When properly compensated $V_m$ steps could be completed in about 20 $\mu$sec (Fig. 1 b).

The experimental chamber was of standard design, with a central measuring electrode 6.2 mm long, and, on either side, guard electrodes 13 mm long. The trough in which the axon was placed was 3 mm deep and 2 mm wide. Partitions on either
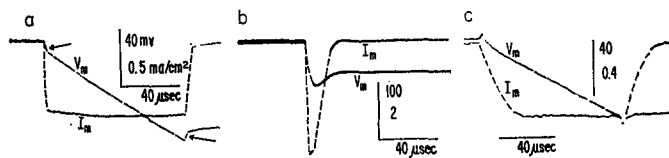


FIGURE 1 a. $V_m$ change in response to an imposed $I_m$ step. Arrows indicate the quick changes in $V_m$ from which $R_s$ was calculated. Connecting lines have been dashed in where the traces did not reproduce well. Fig. 1 b. $I_m$ in response to a $-50$ mv step change of $V_m$. The capacity current transient is over in about 20 $\mu$sec. Fig. 1 c. $I_m$ in response to an imposed ramp change of $V_m$. This calibrating procedure was used to set the current scale factor, in order to compensate for differences in membrane area.

side of the measuring region increased the resistance to longitudinal current flow. The measuring electrode was connected directly to the summing junction of an operational amplifier, whose output was proportional to membrane current. The scale factor, adjustable by a potentiometer, was determined in most experiments by applying a voltage ramp to the membrane $(dV/dt = 1000$ v/sec$)$ and adjusting the potentiometer until the indicated current equaled the value expected for a membrane capacity of 1 $\mu$F/cm² (Fig. 1 c). The potentiometer on a few occasions required a small readjustment after the axon was injected, possibly because axon position or the fluid level in the chamber had changed.

Temperature was measured by a thermistor in one of the guard regions. The thermistor bulb was larger than desirable, and, unfortunately, was not always completely immersed in the bathing medium. This undoubtedly had a detrimental effect on the accuracy of the temperature measurements.

The quaternary ammonium (QA) salts used were methyltriethylammonium iodide $(C_1)$, $n$-propyltriethylammonium iodide $(C_3)$, $n$-butyltriethylammonium iodide $(C_4)$, and $n$-pentyltriethylammonium iodide $(C_5)$. All were obtained from Eastman Kodak Co. For injection, a solution 1–10 mM of the desired compound (in distilled water) was injected in fixed increments at 2 mm intervals through the length of the axon. Total injected volume was about 2 $\mu$l into an axoplasmic volume of about 35 $\mu$l. The diameter of the axon was measured at four points with the axon under

a flat fluid surface. Volume was calculated from the average of these measurements. The scatter of the points in Fig. 3 gives an idea of the accuracy of the calculated concentrations. As a guess, they are in error by a factor of less than 1.5.

Composition of the artificial seawater (ASW) was: $Na^+$, 430 mM; $K^+$, 10 mM; $Ca^{++}$, 10 mM; $Mg^{++}$, 50 mM; $Cl^-$, 560 mM; Tris, 2 mM; pH about 7.5. The high potassium ion solution (440 K) contained $K^+$, 440 mM; $Mg^{++}$, 50 mM; $Ca^{++}$, 10 mM; $Cl^-$, 560 mM; Tris, 2 mM; pH about 7.5.

The experimental records are photographs of the oscilloscope traces. In most cases a number of successive sweeps were superimposed on the frame simply by leaving the camera shutter open. Generally there was an interval of about 2 sec between sweeps.

### RESULTS

*Selective Depression of $g_K$*   The effects of four $TEA^+$ analogues on the voltage clamp currents are shown in Fig. 2. In each case the currents are shown before injection, and after. At the concentrations illustrated all the analogues substantially reduced $g_K$, and for $C_3$-$C_5$ it is clear that $g_{Na}$ is little affected. In one case ($C_4$) $g_{Na}$ is apparently increased after injection, but this is probably an error, as the calibrating circuit (Methods) was not used in this experiment. $C_1$ is probably as selective as $C_3$-$C_5$, but I have no records which demonstrate this clearly. In the $C_1$ experiment illustrated, tetrodotoxin was present in the bathing fluid to eliminate $g_{Na}$.

*Alterations of $g_K$ Time Course*   The time course of $g_K$ shows interesting changes after injection with $C_3$-$C_5$. Instead of increasing smoothly as in the control records, the $K^+$ current ($I_K$) shows a peak (arrows) for large depolarizations (cf. Armstrong, 1966 b; Blaustein, 1968). The prominence of the peak depends both on the analogue injected and on the concentration. It was most prominent with $C_5$ at a concentration of about 0.3 mM (Fig. 8), and was never seen with $C_1$, at any of the concentrations tested (up to 5.7 mM). The origin of the peak will be discussed below.

### The Increase of Blocking Effectiveness with Chain Length

It can be seen in Fig. 2 that the various analogues are not equally potent in suppressing $g_K$. This is illustrated more clearly in Fig. 3 which is a plot of the fraction of $g_K$ that remains after injection as a function of the axoplasmic concentration of the various analogues. In general the concentration required for half-suppression of $g_K$ decreases with increasing chain length, though the data do not make it certain that $C_4$ is more effective than $C_3$.

There is evidence, in the case of $TEA^+$, that one $TEA^+$ ion combines with one blocking site (Armstrong, 1966 b; Hille, 1967 b); i.e., that the process can be represented by

$$\text{Open channel} \underset{l}{\overset{\kappa}{\rightleftharpoons}} TEA^+ \text{ occluded}$$
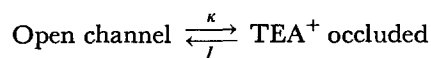
where $\kappa$ (milliseconds$^{-1}$) is a linear function of the TEA$^+$ concentration in the axoplasm:

$$\kappa = b[\text{TEA}^+]_{ax}$$

and $b$ is a constant with units liters mole$^{-1}$ milliseconds$^{-1}$. If this is true for $C_5$,
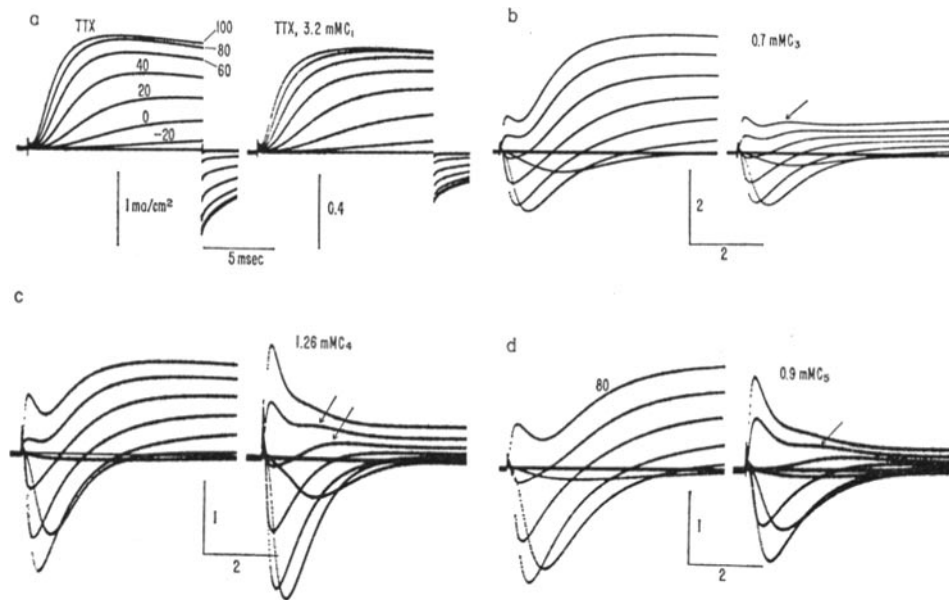


FIGURE 2. $I_m$ in response to step depolarizations from the holding potential, $-60$ mv. Each part (a, b, c, d) shows the currents from an axon before and after injection. $V_m$ during the various steps is shown (in millivolts) in a, and applies also to b, c, and d. Steps were at approximately 2 sec intervals, and traces were superimposed photographically. In a, the bathing medium contained $10^{-7}$ M TTX. Axoplasmic concentrations of the various analogues are indicated. a, 4.0°C; b, 6.6°C; c, 8.0°C; d, 7.4°C, 8.3°C. A different axon was used for each of the four parts of the figure.

for example, the ratio of the potassium current during a large depolarization before and after injection should be given by

$$\frac{I_{\text{K inj}}}{I_{\text{K control}}} = \frac{l}{\kappa + l} = \frac{l}{b[\text{C}_5] + l}$$

The long dashed curve in Fig. 3 that passes through the $C_5$ points was computed from this formula, with $l = 0.28$ msec$^{-1}$, $b = 5.25$ liters mole$^{-1}$ msec$^{-1}$. This curve is in fact specified by setting only the ratio of $l$ to $b$. This particular value of $l$ was chosen for reasons that will become clear in the discussion. The analogous curve (long dashes) for $C_1$ was computed with $l = 9.04$ msec$^{-1}$, $b = 5.25$ liters mole$^{-1}$ msec$^{-1}$. The experimental points are in reasonable

accord with these curves, but the data are not sufficiently precise to exclude, for example, the possibility that two $C_1$ or $C_5$ ions combine with each blocking site (curves with short dashes).
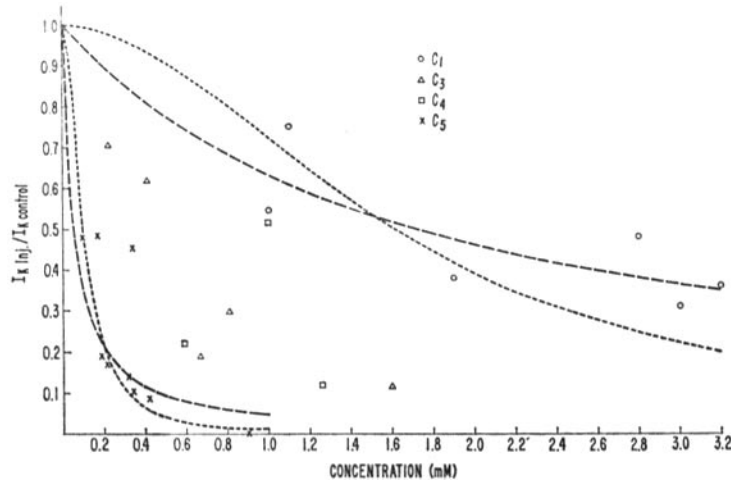


FIGURE 3. The increase of blocking potency with chain length. Ordinate is the fraction of $I_K$ remaining after injection of the various analogues to the axoplasmic concentration given on the abscissa. $I_K$ in this figure only is the $K^+$ current flowing 5 msec after a step depolarization to approximately +50 mv. Long dashed curves were calculated assuming that one ion can block a channel. Short dashed curves assume that two ions are required to block. Collected results with many different axons. Temperature 4–10°C.
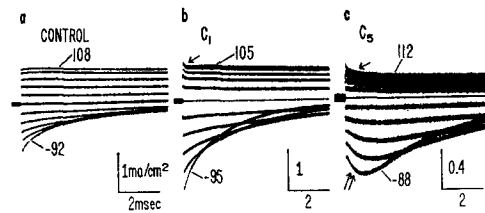


FIGURE 4. $I_m$ for axons in 440 K in response to $V_m$ steps from the resting potential (for a, b, and c, +8 mv, +5 mv, and +12 mv, respectively). $V_m$ step amplitudes were multiples of 20 mv, and the extreme values of $V_m$ are shown in each frame. Current traces were taken at approximately 2 sec intervals and superimposed photographically. a, control, 4.0°C; b, 3 mM $C_1$, 4.0°C; c, 0.9 mM $C_5$, 6.0°C. Three different axons.

*Anomalous or Ingoing Rectification*

All the analogues caused the membrane to be an anomalous or ingoing rectifier; i.e., to have a higher resistance to outward than to inward $K^+$ current. Examples are shown in Fig. 4. In all three cases the fibers were in 440 K, and

were held at the resting potential in that solution until voltage steps were applied that made $V_m$ from 20 to 100 mv positive or negative with regard to the resting potential. From left to right the frames show currents from an uninjected, a $C_1$-, and a $C_5$-injected axon. For the uninjected axon, currents immediately after the step are about the same size whether the step is positive or negative; i.e., the membrane does not rectify the current appreciably at short times. At later times there is outgoing rectification, because the $n^4$ gates close when $V_m$ is made sufficiently negative (Hodgkin and Huxley, 1952 $b$). For both the $C_1$- and the $C_5$-injected axon, on the other hand, the inward currents are larger than the outward shortly after the various steps were applied; i.e., there is ingoing rectification for a time, until the $n^4$ gates close.

$C_5$ causes changes in the time course of the currents in 440 K like those seen previously after TEA$^+$ injection (Armstrong, 1966 $b$). For positive steps the current declines in an exponential or quasi-exponential manner (arrow) to a steady level. As discussed previously (Armstrong, 1966 $b$) this probably means that after the step $C_5$ (or TEA$^+$ in the previous paper) ions enter and stop up an additional fraction of the channels. There is a suggestion of this behavior in the $C_1$ frame (arrow), but it was never seen clearly with $C_1$ regardless of concentration, perhaps because the decline was very fast or very small. For large negative steps the current of the $C_5$ axon increases for a time (double arrow) and then decreases. For TEA$^+$ a similar phenomenon was interpreted as meaning that during the rising phase TEA$^+$ ions are being cleared from the occluded channels faster than the $n^4$ gates of the unoccluded channels are closing (Armstrong, 1966 $b$). Like the decline after positive steps, this increase in current after negative steps was never seen in $C_1$-injected axons. A possible explanation, but not the only one (see Discussion), is that $C_1$ ions leave the channels very quickly, and the process is complete by the time the capacity transient has subsided.

### Increase of $g_K$ on Repolarization

An initial increase of $g_K$ on repolarization, as seen in Fig. 4 c, was not observed in all instances, but only when $V_m$ had been held at a positive value for a sufficient time. Fig. 5 b shows an example for a $C_4$-injected axon. The fiber was in 440 K, held at $V_m = -60$. Shortly after the beginning of the frame $V_m$ was changed to $+100$ mv, and returned to $-60$ mv after 1, 2, or more msec (on successive sweeps). For a maintained depolarization to $+100$ mv, the current showed the usual pattern: a step change in the "leakage" current, followed by an increase, and then a spontaneous decrease in $I_K$. When $V_m$ was returned to $-60$ mv the current was inward in all cases, but current magnitude increased initially only if the preceding depolarization was (in this case) more than a millisecond in duration. The same experiment on an uninjected axon is shown in Fig. 5 a, and it can be seen that $I_K$ decays monotonically on

repolarization regardless of the length of the preceding depolarization. The interpretation given below is that current magnitude increases on repolarization only if a sufficient number of the channels are occluded, and the occluded fraction increases with time after depolarization.

One other feature of the records in Fig. 5 b requires comment: the initial amplitudes (indicated by dots where the traces did not reproduce well) of the inward currents, seen immediately after repolarization, are not proportional
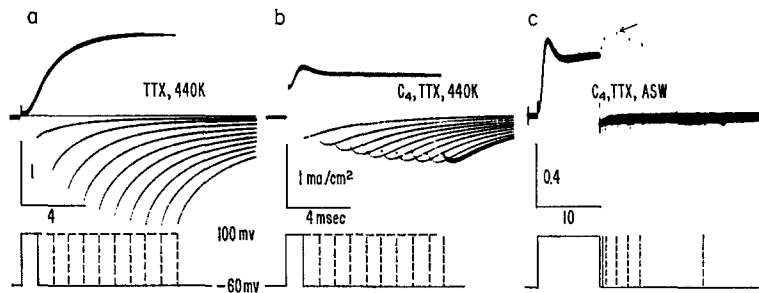


Figure 5 a. $I_m$ for an uninjected axon in 440 K containing $10^{-7}$ M TTX. $V_m$ was held at −60 mv, changed to +100 mv shortly after the beginning of the frame. The upper curve (outward current) gives $I_m$ for $V_m$ = +100. $V_m$ was changed at various times back to −60 mv, and this caused $I_m$ to jump to a negative value (tails below the zero current line). The sequence for the first inward current tail is shown by the solid line in the $V_m$ diagram. Subsequent depolarizing steps of longer duration (broken lines) were applied at approximately 2 sec intervals. Fig. 5 b. Same procedure as in a, but $C_4$ was present in the axoplasm at a concentration of 0.59 mM. a, 5.1°C; b and c, approximately 5°C. a, b, and c were performed on the same axon. Fig. 5 c. $I_m$ in response to $V_m$ changes shown in the diagram. The membrane was depolarized by a step of constant amplitude and duration, and at various times after this step a second very brief step (vertical lines in the $V_m$ diagram) was applied to test membrane conductance, which is seen from the current dots to increase for a time after repolarization from the first step. $V_m$ changes appropriate to the first current dot are shown by solid lines.

to the outward current immediately before repolarization. This suggests that depolarization changes the permeability not only to $K^+$, but to some other ion as well. Little more can be said without further experimentation.

A $g_K$ increase on repolarization could also be seen using suitably injected axons immersed in ASW. In this case the inward currents for injected axons are very small on repolarization, because there is not enough external $K^+$ to carry an appreciable current. For this reason it was necessary to determine membrane conductance by applying a positive voltage step at various times after repolarization. The pulse sequence and the resultant currents are shown in Fig. 5 c. The vertical lines in the potential diagram represent the depolarizing test step, which brought $V_m$ to +100 mv for 0.2 msec. The current during the test step appears as a dot in the current record, and these dots trace out a peak (arrow) of the sort seen in 440 K.

## Inactivation of $g_K$

The up-down behavior of $g_K$ following a step depolarization in a $C_3$-$C_5$–injected axon has a strong resemblance to $g_{Na}$ inactivation (Hodgkin and Huxley, 1952 *a*). Other properties of $g_{Na}$ inactivation are that the fraction of channels inactivated increases as $V_m$ becomes more positive, and that the final level is approached more rapidly as $V_m$ is made more positive. Fig. 6 demonstrates that $g_K$ of a $C_5$-injected axon shares these properties (Armstrong, 1968).
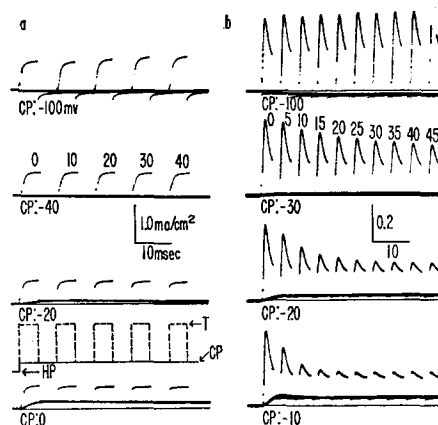


FIGURE 6 a. $I_m$ of an uninjected axon in $10^{-7}$ M TTX in response to the sequence of $V_m$ changes shown in the potential diagram. $V_m$ was held at $-46$ mv ($HP$), then changed at the beginning of the frame to $CP$, whose value is indicated in each frame. After a variable interval at $CP$ (duration of this interval is indicated in milliseconds above the currents in the second frame), $V_m$ was changed to $+90$ mv (T). 2 sec later the same sequence was repeated, but with a different interval at $CP$. $I_m$ during T is about the same, regardless of the duration of the preceding interval at $CP$. Fig. 6 b. Same procedure and the same axon as in a, but the axoplasm contains 0.32 mM $C_5$. $g_K$ inactivates during the interval at $CP$ if $CP$ is positive with respect to the resting potential. a, 7.9°C; b, 9°C.

The pulse sequence is shown in the lower part of Fig. 6 a. $V_m$ was held at the resting potential ($-46$ mv; the axon was in ASW) until the beginning of the frame, when a step was applied that brought $V_m$ to the desired conditioning potential ($CP$). 0–50 msec later a large test depolarization ($T$) was applied, and $V_m$ was then returned to the holding potential. The procedure was repeated 2 sec later, with a different interval between conditioning and test step. The duration of the conditioning pulse is indicated above the current traces in both parts of the figure. After hyperpolarizing conditioning steps of long duration, the maximum current is slightly increased for both the uninjected (Fig. 6 a) and the injected (Fig. 6 b) axon. Thus both display to a limited degree the decrease of inactivation which is seen with $g_{Na}$ upon hyperpolarization. Only the injected axon, on the other hand, shows a significant increase in inactivation following depolarization; i.e., the current peaks are

smaller after a depolarizing conditioning step. As with $g_{Na}$ inactivation, the rate and the extent of inactivation are greater (up to a point) as $V_m$ is made more positive.

Thus it seems proper to speak of $g_K$ inactivation in $C_b$-injected fibers, since the phenomenon has all the essential features of $g_{Na}$ inactivation. There is, however, a possible difference in the time course of inactivation in the two cases. In Fig. 7, which shows the experiment of Fig. 6 b at higher sweep speed, the envelope of the $I_K$ peaks is S-shaped. This may not be true for a similar experiment on $g_{Na}$ (see below).
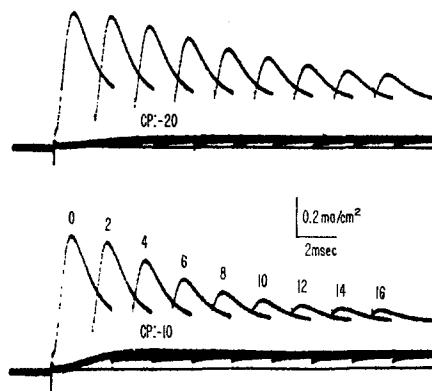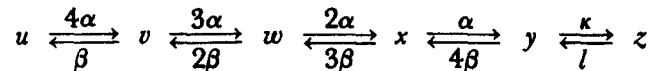


FIGURE 7. The experiment of Fig. 6 b at faster sweep speed. The envelope of the $I_m$ peaks is sigmoid. 9°C.

## DISCUSSION

The phenomena described above give a substantial amount of information about the interaction of QA ions and the potassium channels. Similar phenomena observed after TEA$^+$ injection were accounted for by a kinetic scheme with the following essential features (Armstrong, 1966 b).

1. TEA$^+$ does not affect the rate constants, $\alpha$ and $\beta$, used by Hodgkin and Huxley (1952 b) to describe the kinetics of the $n^4$ gate.

2. TEA$^+$ does not change $g_K$ (Hodgkin and Huxley, 1952 b).

3. TEA$^+$ can occlude only those channels with open $n^4$ gates.

4. After a sufficient recovery period at the resting potential, all the channels are free of TEA$^+$.

5. A channel is either fully open or fully closed.

6. TEA$^+$ blocks channels at a rate that varies with its axoplasmic concentration. The rate may also depend on other factors, e.g. $V_m - V_K$.

7. Making $V_m$ negative with respect to $V_K$ (i.e., driving potassium current inward) clears the channels of TEA$^+$. It is not certain whether this results from an increase in the exit rate or a decrease in the entry rate.

A scheme which has the same general features (if the constants are properly

adjusted) and which can be used to account for the data presented above is the following:

$$u \underset{\beta}{\overset{4\alpha}{\rightleftharpoons}} v \underset{2\beta}{\overset{3\alpha}{\rightleftharpoons}} w \underset{3\beta}{\overset{2\alpha}{\rightleftharpoons}} x \underset{4\beta}{\overset{\alpha}{\rightleftharpoons}} y \underset{l}{\overset{\kappa}{\rightleftharpoons}} z$$

In this scheme, $g_K$ is proportional to $y$, and the number of QA-occluded channels is proportional to $z$. This is identical to the TEA$^+$ scheme, but $XC$ of the previous paper has been separated into states $u$, $v$, $w$, and $x$ in order to reproduce the S-shaped rise of $g_K$ following depolarization. This presentation is similar to Fitzhugh's (1965) in some respects, and it was he who pointed out to me that it is equivalent to the Hodgkin-Huxley equations for $g_K$, when the rate constants are as shown. $u$, $v$, $w$, $x$, and $y$ represent channels with, respectively, 4, 3, 2, 1, and 0 of the hypothetical particles of Hodgkin and Huxley (1952 $b$) in blocking position. $y$ is thus equivalent to their $n^4$. $\alpha$ and $\beta$ (equivalent to the $\alpha$ and $\beta$ of Hodgkin and Huxley) are respectively the rate constants for a single particle leaving and entering the blocking position. Since in state $u$, for example, there are four particles in blocking position, the rate constant for conversion of state $u$ to state $v$ is four times the rate constant for a single particle leaving position; i.e., $4\alpha$. Similar reasoning leads to the other rate constants given in the diagram.

For the normal axon (i.e., state $z$ omitted, or $\kappa = 0$) the model works as follows. At the resting potential $\beta$ is large and $\alpha$ is small, so few of the channels are in state $y$, many (or, for $\alpha = 0$, all) are in state $u$. If the membrane is depolarized, $\alpha$ becomes large, $\beta$ small, so that many channels progress from left to right in the diagram, and $y$ begins to increase, but after a time lag, since the channels must progress from $u$ to $v$ to $w$, etc., before reaching $y$. $y$ thus increases with an S-shaped time course to a steady level that is maintained until $\alpha$ and $\beta$ are changed. On repolarization $\beta$ becomes large again, $\alpha$ small, and $y$ decays not with an S-shaped time course, but in a quasi-exponential manner (or, for $\alpha = 0$, exponential). The effect of QA ions can be simulated by adding state $z$ (TEAC in the previous paper). State $z$ represents a channel with open $n^4$ gate that is plugged by a QA ion.

### Application to the Currents That Follow Depolarizing Steps

This model was first fitted to the currents that follow step depolarizations in normal and $C_5$-injected axons. The fitting procedure (for details, see below) consisted essentially of determining $\alpha$, $\beta$, and $g_K$ by fitting the preinjection curves with $\kappa = 0$; and then holding $\alpha$, $\beta$, and $g_K$ fixed (except for temperature corrections) while $\kappa$ and $l$ were varied to obtain a good fit to the postinjection curves. There are two points of special note in this procedure: the assumption that $\alpha$, $\beta$, and $g_K$ are unaffected by $C_5$, and the fact that all five

constants can be uniquely determined. The procedure makes use of the first five points mentioned above, and a good fit will thus provide a measure of support for the validity of these points.

The kinetic scheme of the arrow diagram can be described by six linear first-order differential equations of the type (taking $y$ as an example)

$$dy/dt = -\kappa y - 4\beta y + \alpha x + lz.$$

Using the condition

$$u + v + w + x + y + z = 1,$$

one differential equation can be eliminated, and it is then possible to obtain a single, equivalent fifth-order equation in $y$, or, if $z$ is omitted, a fourth-order equation. It can be shown that

$$y = n^4 = [n_\infty - (n_\infty - n_o)e^{-t/\tau}]^4$$

satisfies the fourth-order equation ($z$ omitted), demonstrating the equivalence of $y$ to $n^4$ of the Hodgkin-Huxley equations.

For computational purposes, the six first-order equations were programmed on an analogue computer, and the fitting procedure was then quite straightforward. A rather low value, $-50$ mv, was selected for $V_K$, to allow for accumulation of $K^+$ in the Schwann cell space. This value was probably too low for small depolarizations. Ideally, conductance-time rather than current-time curves should be fitted in order to eliminate this problem. $\beta$ was assumed equal to zero for $V_m = +90$ mv, and $\bar{g}_K$ was calculated from the current and the driving force at this voltage. Leakage current was assumed to be a linear function of $V_m$, with $V_{leak} = -60$ mv, and $g_{leak} = 0.3$ mmho. $\alpha$ was assumed to be zero at the holding potential, which is equivalent to saying that $u = 1$ in the steady state at this potential. The problem was scaled so that the computer output was proportional to $I_K$. Having fixed $V_K$ and $\bar{g}_K$, $\alpha$ and $\beta$ were varied with $\kappa = 0$ until the computer curve matched the experimental curve obtained before injection. The $\alpha$ and $\beta$ values so obtained for a given depolarization were then held fixed (except for temperature correction, assuming a $Q_{10}$ of three), and $\kappa$ and $l$ were varied to fit the postinjection curve for the same depolarization.

The degree of success in fitting the curves from two experiments can be judged from Fig. 8, where the dots are experimental points and the curves are computer-drawn. The values of the various constants used for fitting each curve are given in Table I. The fit to the preinjection curves (a and c) is fairly good, but, as pointed out by Cole and Moore (1960), $g_K$ experimentally rises after a longer time lag than the Hodgkin-Huxley equation can provide for. The fit to the postinjection curves is fair in places and very good in others.

In Fig. 8 b, the computer curves peak a bit too late for large depolarizations. The discrepancy is not great, and could arise, for example, from improper setting of the potentiometer that determines the scale factor for the current, or from having underestimated the postinjection temperature (see Methods).
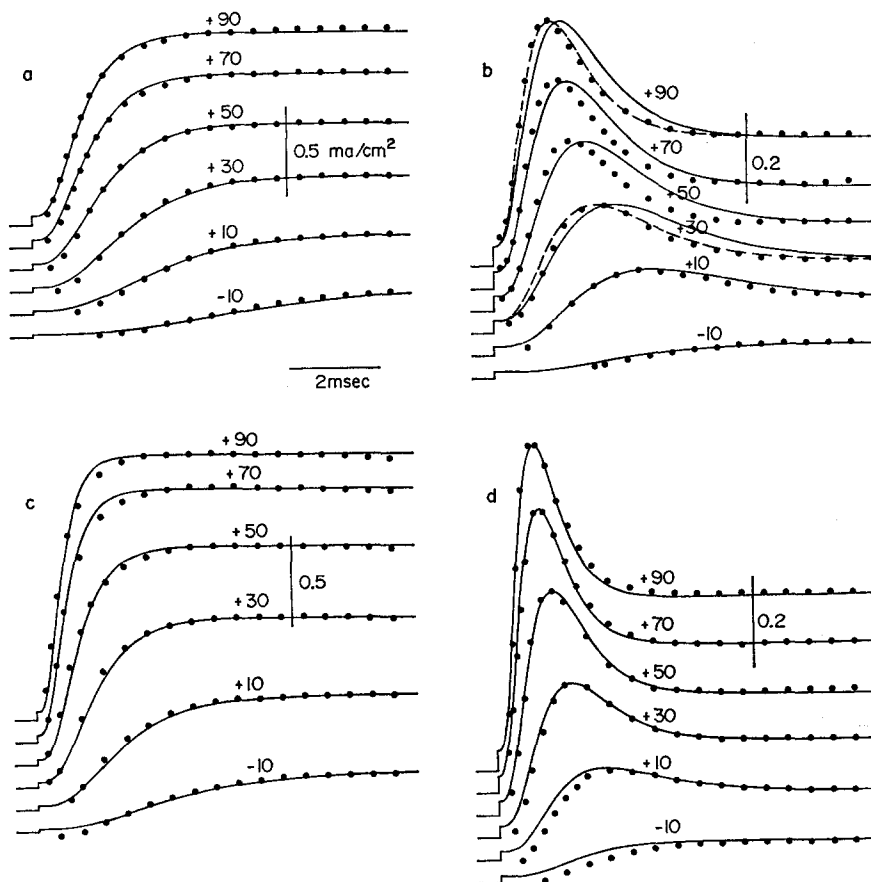


FIGURE 8. Experimental currents (points), and computer-drawn curves, generated from the kinetic scheme shown in Discussion. 8 a. Preinjection currents of an axon in $10^{-7}$ M TTX, and curves drawn to fit them, using the values for the various constants that are shown in Table I. 8 b. As in a, but the axoplasm contains 0.32 mM $C_5$. The dashed curve assumes that the temperature was 1.5°C higher than measured. c and d, another experiment. $C_5$ concentration in d was approximately 0.3 mM.

The dashed curves, which fit the data very well, are calculated on the assumption that temperature after injection was 1.5 °C higher than recorded, and that the rate constants have a $Q_{10}$ of three. In Fig. 8 d, the computer curves are an excellent match to the points for large depolarizations. For small depolarizations there is a discrepancy which arises at least in part from a

residual trace of sodium current, evident from the fact that the current points initially go below the zero line. In general, however, the fit of model to data seems very good, and there is no question that the model behaves much as required.

TABLE I

| | $V_m$ | $[C_i]_{ax}$ | $\alpha$ | $\beta$ | $\kappa$ | $l$ | $\bar{g}_K$ | $V_K$ | $T$ |
|---|---|---|---|---|---|---|---|---|---|
| | $mv$ | $mM$ | $msec^{-1}$ | $msec^{-1}$ | $msec^{-1}$ | $msec^{-1}$ | $\dfrac{mmhos}{cm^2}$ | $mv$ | $°C$ |
| a. | +90 | 0 | 1.65 | 0 | 0 | — | 7.46 | −50 | 7.6 |
| | +70 | 0 | 1.45 | 0 | 0 | — | 7.46 | −50 | 7.6 |
| | +50 | 0 | 1.15 | 0 | 0 | — | 7.46 | −50 | 7.6 |
| | +30 | 0 | 0.85 | 0 | 0 | — | 7.46 | −50 | 7.6 |
| | +10 | 0 | 0.65 | 0 | 0 | — | 7.46 | −50 | 7.6 |
| | −10 | 0 | 0.35 | 0.015 | 0 | — | 7.46 | −50 | 7.6 |
| b. | +90 | 0.32 | 1.85* | 0 | 0.84 | 0.254 | 7.46 | −50 | 8.8 |
| | | | 2.14‡ | | 0.99‡ | 0.301‡ | | | |
| | +70 | 0.32 | 1.62 | 0 | 0.86 | 0.215 | 7.46 | −50 | 8.8 |
| | +50 | 0.32 | 1.28 | 0 | 0.74 | 0.187 | 7.46 | −50 | 8.8 |
| | +30 | 0.32 | 0.95 | 0 | 0.64 | 0.175 | 7.46 | −50 | 8.8 |
| | | | 1.13‡ | | 0.76‡ | 0.208‡ | | | |
| | +10 | 0.32 | 0.73 | 0 | 0.55 | 0.170 | 7.46 | −50 | 8.8 |
| | −10 | 0.32 | 0.39 | 0.017 | 1.4 | 0.360 | 7.46 | −50 | 8.8 |
| c. | +90 | 0 | 3.1 | 0 | 0 | — | 11.3 | −50 | 11.2 |
| | +70 | 0 | 2.6 | 0 | 0 | — | 11.3 | −50 | 11.2 |
| | +50 | 0 | 1.9 | 0 | 0 | — | 11.3 | −50 | 11.2 |
| | +30 | 0 | 1.40 | 0 | 0 | — | 11.3 | −50 | 11.2 |
| | +10 | 0 | 0.95 | 0.015 | 0 | — | 11.3 | −50 | 11.2 |
| | −10 | 0 | 0.55 | 0.066 | 0 | — | 11.3 | −50 | 11.2 |
| d. | +90 | Approximately 0.3 | 3.30§ | 0 | 1.6 | 0.500 | 11.3 | −50 | 11.8 |
| | +70 | 0.3 | 2.77 | 0 | 1.7 | 0.458 | 11.3 | −50 | 11.8 |
| | +50 | 0.3 | 2.02 | 0 | 1.5 | 0.380 | 11.3 | −50 | 11.8 |
| | +30 | 0.3 | 1.48 | 0 | 1.45 | 0.38 | 11.3 | −50 | 11.8 |
| | +10 | 0.3 | 1.01 | 0.016 | 1.39 | 0.34 | 11.3 | −50 | 11.8 |
| | −10 | 0.3 | 0.59 | 0.070 | 1.75 | 0.37 | 11.3 | −50 | 11.8 |

* To correct for temperature increase, $\alpha$ and $\beta$ from a were multiplied by 1.1.
‡ For dashed curve in Fig. 8 b.
§ To correct for temperature increase, $\alpha$ and $\beta$ from c were multiplied by 1.06.

The current curves fitted above are not perfect replicas of the conductance curves which they have been taken to represent, because of $K^+$ accumulation in the Schwann cell space. For this reason the values obtained for the various constants must be treated with some reservation. Over the range studied, $\kappa$ and $l$ change very little, declining slightly as $V_m$ goes negative, and then suddenly jumping in value between $+10$ and $-10$ mv (Table I b and d).

This sudden rise may well be an error: the curves are not very good fits to begin with; and the residual sodium current (largest in amplitude at about $-10$ mv) would, by partially cancelling an oppositely directed peak in $I_K$, and thus flattening the $I_K$ curve, lead to the use of a falsely high $\kappa$ value (see Fig. 9).

The near constancy of $\kappa$ over a wide range in Table I d, suggests that the entry rate of $C_5$ in this experiment may have been limited by the rate of $C_5$ diffusion to the channel mouths. In neither experiment is there the increase in the $\kappa:l$ ratio as $V_m$ approaches $V_K$ that is invoked below to explain anomalous rectification. This is not particularly surprising, as the experiments of Armstrong and Binstock (1965) indicate that most of the change in this ratio takes place in a fairly narrow voltage range about $V_K$, while the nearest determination here is 40 mv away from the assumed $V_K$.

### Application to other QA Ions

In the scheme given above, the steady-state fraction of the channels in states $y$ and $z$ depends only on the $\kappa:l$ ratio (if $\beta = 0$). This final level is approached with varying degrees of overshoot: as $l$ decreases ($\kappa:l$ ratio constant) the overshoot grows larger. This is illustrated in the computed curves of Fig. 9. Three of the curves approach the same final level, and as $l$ goes from small to large the curves at first resemble the experimental $C_5$ curve (Figs. 8 b and d), and end by resembling the $C_1$ curve (Fig. 2 a). Thus, the differences in time course with the various analogues can be explained by saying that $l$ gets progressively smaller as —$CH_2$— groups are added. On the other hand, $b$, the proportionality constant between $\kappa$ and QA concentration, is not greatly changed by altering chain length, as evidenced by comparison of the values found above for $C_5$ with the values found previously for $TEA^+$: at equal concentrations, $\kappa$ would be about the same for both. Fig. 3 can be explained on the same basis, that $b$ (or $\kappa$ at fixed QA concentration) is independent of chain length, while $l$ is smaller for longer chain lengths. The data, of course, do not exclude some variation of $b$ with chain length, but it must be small in comparison with the change in $l$.

From the results with $C_1$-$C_5$ one can straightforwardly predict a still more prominent overshoot with longer chain lengths. The limiting case, for $l = 0$, is illustrated in Fig. 9.

The decrease of $l$ with added —$CH_2$— groups has a simple physical interpretation. The binding site in the channel, be it a pore or a carrier, apparently has a hydrophobic component as well as the polar component usually postulated and the added —$CH_2$— groups bond to this hydrophobic component. Hydrophobic bonding could more than account for the decrease in $l$ that comes from the addition of —$CH_2$— groups. Moving one such group from a nonpolar to an aqueous medium requires 860 cal/mole (Davies and Rideal,
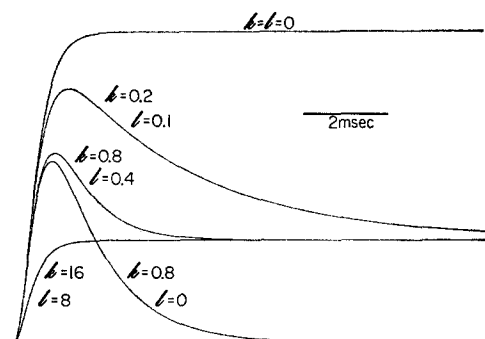
FIGURE 9. Theoretical $g_K$ curves (ordinate, in arbitrary units), for the $\kappa$ and $l$ values shown. $\alpha$ and $\beta$ in all cases were 3.1 msec$^{-1}$ and 0. The curves show that for a constant final level, the degree of overshoot increases as $l$ grows smaller; i.e., inactivation becomes more prominent.

1963). At room temperature, subtracting this quantity from the activation energy in the Arrhenius equation increases the affected rate constant by a factor of 4.1. Thus, each —CH$_2$— group removed from the chain would increase the rate constant, $l$, by a factor of 4.1, if the group formed an effective hydrophobic bond with the blocking site; and in going from C$_5$ to C$_1$ $l$ would increase by a factor of 300. The observed factor, if $b$ is independent of chain length, is more nearly 30 (see Fig. 3), or a factor of roughly 2.5 per —CH$_2$— removed. This presumably means that not all the —CH$_2$— groups form fully effective hydrophobic bonds.

*Anomalous Rectification*

As discussed above in point (7), anomalous or ingoing rectification with this scheme can be accomplished by supposing that the $\kappa$:$l$ ratio increases as $V_m$-$V_K$ is made positive, and decreases as it is made negative. The result is that a greater fraction of the channels are in state $z$ when $V_m$-$V_K$ is positive, and a lesser fraction when it is negative. If these constants are very large, the steady-state distribution is achieved quickly and the rectification is established, apparently, instantaneously, or too quickly to detect. This may well be the case with C$_1$, for which $l$ is large, and $\kappa$ is large because a high concentration of C$_1$ must be used to achieve an appreciable effect. If $\kappa$ and $l$ are small, as with C$_5$ at low concentration, transients such as those in Fig. 4 c are seen, which indicate movement of the blocking ion.

*Application to the Transient Increase of $g_K$ on Repolarization*

As noted, making $V_m$ negative with respect to $V_K$ tends to clear the channels of QA ions and this is responsible for the transient increase in $g_K$ when $V_m$ is returned to —60 mv (Figs. 5 b and c). The scheme also predicts that the increase will be present only after a depolarization of sufficient duration. Net rate $z$ → $y$ must be larger than net rate $y$ → $x$ for the increase to occur, and $z$ → $y$ increases with $z$. $z$ is small immediately after depolarization, but grows with time, leading to the observed result.

A sample calculation is given in Fig. 10. Since there is no good evidence on the behavior of the constants, $\kappa$ and $l$, in the neighborhood of $V_K$, the choice of rate constants for simulating repolarization is rather arbitrary, and the intent of the calculation is purely qualitative. Reasons for believing $\kappa = 0$ on repolarization (as assumed in the calculation) were given previously (Armstrong, 1966 b). Other constants were taken as $\alpha = 0$, $\beta = 0.2$ msec$^{-1}$, $l = 1.2$ msec$^{-1}$. The constants for depolarization are from the $+90$ mv curve of Fig. 8 d. Leakage current was omitted. Events on repolarization may well be more complicated than assumed here, but the computed curves nonetheless reproduce many of the features of Fig. 5 b. They do not reproduce the continued
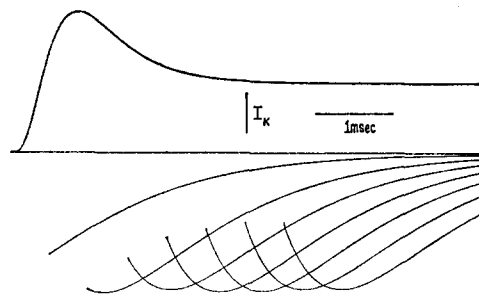


FIGURE 10. Theoretical $I_K$ curves (arbitrary units) to simulate the results of step depolarization (curve above the zero line) with repolarization at various times after, as in Fig. 5 b. The model correctly predicts that $I_K$ magnitude will increase after repolarization only if the preceding depolarization was of sufficiently long duration. During depolarization, $\alpha = 3.3$ msec$^{-1}$, $\beta = 0$, $\kappa = 1.6$ msec$^{-1}$, $l = 0.5$ msec$^{-1}$. After repolarization, $\alpha = 0$, $\beta = 0.2$ msec$^{-1}$, $\kappa = 0$, $l = 1.2$ msec$^{-1}$.

increase in initial amplitude of the inward currents after the outward current has begun to diminish (see Results).

At this point it should be noted that some, but not all, the findings with $C_1$ could be explained by supposing that $C_1$ ions can enter channels with closed $n^4$ gates. Thus the absence of overshoot in the $I_K$ records following step depolarization (e.g. Fig. 2 a) could mean that $C_1$ was equilibrated between axoplasm and blocking sites at the resting potential even though the $n^4$ gates were closed. The absence of a current increase after repolarization in Fig. 4 b could mean that the $n^4$ gates of the occupied channels closed despite the presence of $C_1$. In short, if these suppositions were correct, $C_1$ would simply have the effect of decreasing $g_K$. This is conceivable, but such an effect would leave unexplained the ingoing rectification observed when $C_1$ is present. Ingoing rectification, and the absence of any other signs of $C_1$ movements must mean that such movements are very rapid, and one is led back to the previous hypothesis, which accounts for all the data: that $l$ for $C_1$ is very large, and therefore $\kappa$ must be large for $C_1$ to have an appreciable effect; i.e., the $C_1$ concentration must be high.

*The Effects of Conditioning Steps*

The kinetic scheme proposed above gives a good facsimile of the behavior of $g_K$ in $C_5$-injected axons subjected to conditioning steps, as can be seen by comparing the computed curves of Fig. 11 with the experimental curves of Figs. 6
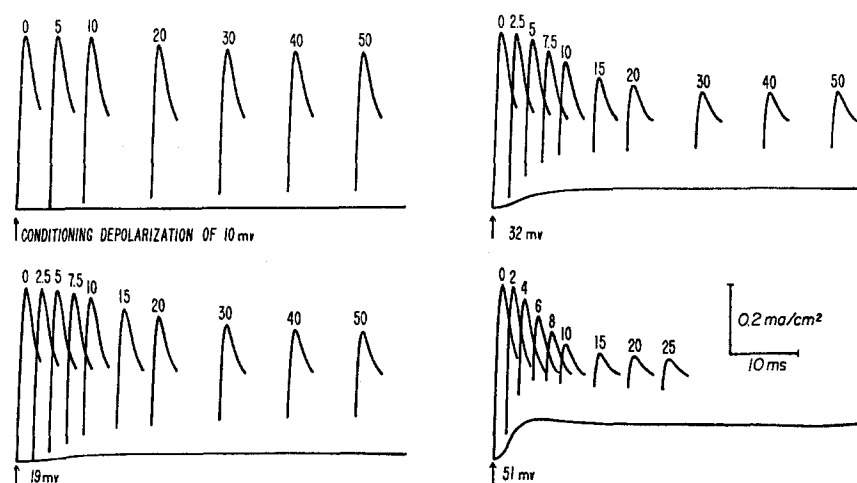


FIGURE 11. Theoretical $I_K$ curves generated by the kinetic model to simulate the experiment of Figs. 6 b and 7. Values of the constants used in the calculation are given in Table II. The model correctly predicts that inactivation will be faster and more complete as $V_m$ during the conditioning step is made more positive, and that the envelope of the current peaks will be sigmoid.

TABLE II

| Depolarizing step | $\alpha$ | $\beta$ | $\kappa$ | $l$ | $\bar{g}_K$ | $V_K$ |
|---|---|---|---|---|---|---|
| *mv* | *msec⁻¹* | *msec⁻¹* | *msec⁻¹* | *msec⁻¹* | | |
| 10 | 0.095 | 0.096 | 0.55 | 0.17 | 7.46 | −50 |
| 19 | 0.150 | 0.072 | 0.55 | 0.17 | 7.46 | −50 |
| 32 | 0.241 | 0.071 | 0.55 | 0.17 | 7.46 | −50 |
| 51 | 0.419 | 0.069 | 0.55 | 0.17 | 7.46 | −50 |
| 150 | 1.85 | 0 | 0.84 | 0.254 | 7.46 | −50 |

and 7. Because $\alpha$ and $\beta$ were not determined for small depolarizations, but instead, were taken from Hodgkin and Huxley (1952 *b*), the computed curves are not intended as precise replicas of the experimental curves. The resemblance nonetheless is close. Both sets of curves show that inactivation is more rapid and more complete with larger depolarizations. Also, the envelope of the computed peaks has the S-shape seen in Fig. 7, indicating that a channel can be inactivated (or QA occluded) only after its $n^4$ gate has opened.

Table II gives the constants used in calculating Fig. 11.

Again it can be predicted that longer chain compounds having lower values of $l$ will make the effects of conditioning steps still more pronounced.

### Comparison with Other Models

It is clear from the above that the model presented here will reproduce most of the phenomena that have been recorded, but one might ask if it is better able to do so than an equation similar to the Hodgkin-Huxley equation for $g_{Na}$; i.e., an equation with $n^4$ multiplied by an inactivation factor. There is little doubt that such an equation could fit the currents following depolarizing steps, because the transient observed is similar to the $I_{Na}$ transient for which the Hodgkin-Huxley $g_{Na}$ equations were designed. Also, the increase of $g_K$ on repolarization could probably be fitted, simply by allowing recovery from inactivation to proceed rapidly. There are two points, however, where such an equation would not fit. One is the time course of inactivation, which in the present case is sigmoid (Fig. 7) and could not be reproduced by an H-H–like equation unless the inactivation factor were somehow modified. Second, $h$ in their equations is dependent on voltage and time, and independent of equilibrium potential $(V_{Na})$. The fraction of the channels inactivated by QA ions, on the other hand, unquestionably depends on the equilibrium potential for potassium ion. The model of Hoyt (1963, 1968) will reproduce the sigmoid time course of inactivation, but again, all the variables in her model are independent of equilibrium potential.

The model presented here is of the class which Hoyt calls "coupled;" i.e., the $n^4$ gate and the inactivation gate are not independent. The sigmoid time course of inactivation lends support to this type of model, but certainly does not prove it to be correct (Hoyt, 1968).

### Resistance and Surface Density of the Channels

The $\kappa$ values determined above can be used to calculate the rate at which $K^+$ ions move through their channels in the membrane. The method, and the assumptions required, were given previously (Armstrong, 1966 b; cf. Cole, 1968). Taking $\kappa = 0.84$ msec$^{-1}$ (from the depolarization to $+90$ mv, Table I b), the calculation shows that one $K^+$ ion enters each channel (on the average) every 1.2 $\mu$second, in good agreement with the figure obtained for TEA$^+$ (one $K^+$ ion every 1.7 $\mu$second). A monovalent ion flux of this magnitude constitutes an electric current of $1.3 \times 10^{-13}$ amp. Taking the driving force at $V_m = +90$ mv as 140 mv, the resistance of a single channel is approximately $10^{12}$ ohms. This is roughly 100 times greater than the resistance of a $K^+$-filled tube (one-third molar) of plausible single channel dimensions (radius 4.5 A; length 100 A).

The surface density of the channels can be obtained by dividing the total current by the current per channel. For a total current of 1 ma/cm$^2$ (Fig.

8 a) and a current per channel of $1.3 \times 10^{-13}$ amp, the channel density must be about 70 channel/$\mu^2$, again in close agreement with the TEA$^+$ figure (67 channels/$\mu^2$). The same calculation can be made using the $\kappa$ value for other depolarizations, provided one knows what fraction of the channels are open for each depolarization. Because the value of $V_K$ used above was too low for small depolarizations, the open fraction was in general overestimated. Better estimates, taken from (unpublished) step conductance measurements and combined with the values of Table I b give very nearly the same total (i.e., open + unopen) channel density for all except the depolarization to $-10$ mv, for which, as noted, the $\kappa$ value may be in error. In contrast, the $\kappa$ values in Table I d give a smaller total channel density for smaller depolarizations. The near constancy of $\kappa$ with $V_m$ in this experiment may mean that the rate of $C_s$ entry into the channels was diffusion-limited, and hence did not very accurately reflect the K$^+$ entry rate. The maximum error introduced in this way would be the factor by which the diffusion coefficient for K$^+$ exceeds that for $C_s$; i.e., the K$^+$ entry rate might be underestimated by a factor of roughly three. Another possible error in the calculation lies in the assumption that $C_s$ and K$^+$ enter the channels with equal ease.

As it stands, the channel density figure is in reasonable agreement with the channel density estimates obtained by others. Chandler and Meves (1965), unable to detect a current caused by the movement of carriers or gating particles in squid nerve, estimated that Na$^+$ channels must be less dense than $100/\mu^2$. Moore et al. (1967) estimate that for lobster nerve there are less than 13 channels/$\mu^2$. This agreement in order of magnitude may, of course, prove fortuitous.

### Applicability to $g_{Na}$ Inactivation

One wonders, of course, whether a model of the general type presented here is applicable to $g_{Na}$ inactivation. The balance of the evidence at present seems to be against it. Chandler et al. (1965) in response to a model proposed by Hoyt (1963; see also Hoyt, 1968), specifically considered whether or not $g_{Na}$ inactivation begins after a time lag, and reaffirmed the original description of Hodgkin and Huxley: that inactivation has an exponential time course, and sets in with no time lag. However, their experimental procedure was somewhat more complicated than that of Hodgkin and Huxley (1952 a), and it would be worthwhile to repeat the original experiments using TEA$^+$ to eliminate $I_K$. This seems particularly necessary in view of unpublished observations by Taylor[1] that indicate a sigmoid time course for inactivation. Also of interest is the finding of Chandler and Meves (1966) that $g_{Na}$ inactivation is less complete for very large depolarizations when internal Na$^+$ is high. Since both a large depolarization and raising the internal Na$^+$ increase outward $I_{Na}$, this

[1] Taylor, R. E. Unpublished observations.

could mean that outward $I_{Na}$ clears the $Na^+$ channels in the same way that inward $I_K$ clears the $K^+$ channels.

### Comparison with Gating Phenomena in Other Excitable Membranes

One of the major interests of this work is that QA ions can induce permeability gates in squid membrane that resemble naturally occurring gates in other tissues. An intriguing example is the similarity of $C_5$ inactivation to the native $g_K$ inactivation seen in the puffer fish (Nakajima and Kusano, 1966; Nakajima, 1966). Thus one might speculate that puffer neurons contain a QA-like substance, with concentration and properties such that $\kappa = 0.15$ msec$^{-1}$ and $l = 0.01$ msec$^{-1}$. This would provide rather complete inactivation with about the right time course. Movement of the hypothetical blocking particles would be so slow with these rate constants that ingoing rectification would not be apparent, and, in fact, it is not observed in puffer neurons.

QA-like gates are also seen in muscle fiber membranes. Already cited is the similarity between $TEA^+$-induced ingoing rectification in squid and the ingoing rectification in muscle. As another example, Noble and Tsien (1968) have described channels in Purkinje fibers that have voltage-sensitive gates (governed by a variable called $s$, that has many properties similar to $n^4$) and in addition have ingoing rectifier properties; i.e., just as in squid with $TEA^+$, each channel is an ingoing rectifier always closed to outward current, and open to inward current only if the voltage-sensitive gate is open. Similar properties have been observed in skeletal muscle (Adrian, Chandler, and Hodgkin, cited in Noble and Tsien, 1968). Finally, skeletal muscle fibers have an inactivation of $g_K$ that is quite slow, but possibly occurs by a mechanism of the type described here. It is conceivable that muscle cells acquire both properties, ingoing rectification and $g_K$ inactivation, through the metabolism of one class of $TEA^+$-like compounds; and that the blocking molecules for the two functions differ from each other only in the number of $-CH_2-$ groups found in a side chain.

### Comparison with Drug Effects on Other Nerve Membranes

Hille (1967 *b*) has demonstrated convincingly that the effect of $TEA^+$ on the node of myelinated fibers from *Rana pipiens* can be described as a simple reduction of $\bar{g}_K$. Equally convincing are the experiments of Koppenhöfer (1967) which show that the effect on the node of *Xenopus laevis* is more complex. This must certainly be a species difference. Both species differ from squid and in neither case does the model given above seem applicable without severe modification. For one thing, $TEA^+$ apparently acts on the outside of nodal membrane. Also, unlike squid, nothing in the records suggests that $TEA^+$ has access to the blocking sites only when the $n^4$ gates are open. Finally, unlike squid, $TEA^+$ binding is unaffected by changing $V_m - V_K$ (Koppenhöfer, 1967).

Under the influence of tropine esters applied externally, $g_K$ of the lobster nerve shows some degree of inactivation (Blaustein, 1968). This action could be accounted for by saying, as for QA ions, that the blocking sites to which the ester binds are accessible only when the $n^4$ gates of the channels are open.

## REFERENCES

ADRIAN, R. H., W. K. CHANDLER, and A. L. HODGKIN. 1968. Voltage clamp experiments in striated muscle fibers. *J. Gen. Physiol.* **51** (5, Pt. 2):188s.

ARMSTRONG, C. M. 1966 *a*. Interference of injected tetra-*n*-propylammonium bromide with outward Na⁺ current flow in the squid giant axon. *Nature (London).* **211**:322.

ARMSTRONG, C. M. 1966 *b*. Time course of TEA⁺-induced anomalous rectification in squid giant axon. *J. Gen. Physiol.* **50**:491.

ARMSTRONG, C. M. 1968. Induced inactivation of the potassium permeability of squid axon membranes. *Nature (London).* **219**:1262.

ARMSTRONG, C. M., and L. BINSTOCK. 1964. The effects of several alcohols on the properties of the squid giant axon. *J. Gen. Physiol.* **48**:265.

ARMSTRONG, C. M., and L. BINSTOCK. 1965. Anomalous rectification in the squid giant axon injected with tetraethylammonium chloride. *J. Gen. Physiol.* **48**:859..

BLAUSTEIN, M. P. 1968. Action of certain tropine esters on voltage-clamped lobster axon. *J. Gen. Physiol.* **51**:309.

CHANDLER, W. K., A. L. HODGKIN, and H. MEVES. 1965. The effect of changing the internal solution on sodium inactivation and related phenomena in giant axons. *J. Physiol. (London).* **180**:821.

CHANDLER, W. K., and H. MEVES. 1965. Voltage clamp experiments on internally perfused giant axons. *J. Physiol. (London).* **180**:788.

CHANDLER, W. K., and H. MEVES. 1966. Incomplete sodium inactivation in internally perfused giant axons from *Loligo forbesi. J. Physiol. (London).* **186**:121P.

COLE, K. S. 1968. Membranes, Ions and Impulses. University of California Press, Berkeley. P. 533.

COLE, K. S., and J. W. MOORE. 1960. Potassium ion current in the squid giant axon: dynamic characteristics. *Biophys. J.* **1**:1.

DAVIES, J. T., and E. K. RIDEAL. 1963. Interfacial Phenomena. Academic Press, Inc., New York. 2nd edition.

EHRENSTEIN, G., and D. L. GILBERT. 1966. Slow changes in potassium permeability in squid giant axon. *Biophys. J.* **6**:553.

FITZHUGH, R. 1965. A kinetic model of the conductance changes in nerve membrane. *J. Cell. Comp. Physiol.* **66** (Suppl. 2):111.

HAGIWARA, S., and N. SAITO. 1959. Voltage-current relations in nerve cell membrane of *Onchidium verruculatum. J. Physiol. (London).* **148**:161.

HILLE, B. 1967 *a*. Quaternary ammonium ions that block the potassium channel of nerves. Abstracts of the Biophysical Society 11th Annual Meeting. Houston, Texas. P. 19.

HILLE, B. 1967 *b*. The selective inhibition of delayed potassium currents in nerve by tetraethylammonium ion. *J. Gen. Physiol.* **50**:1287.

HODGKIN, A. L., and A. F. HUXLEY. 1952 *a*. The dual effect of membrane potential on sodium conductance in the giant axon of *Loligo. J. Physiol. (London).* **116**:497.

HODGKIN, A. L., and A. F. HUXLEY. 1952 *b*. A quantitative description of membrane current and its application to conductance and excitation in nerve. *J. Physiol.* (*London*). **117**:500.

HOYT, R. C. 1963. The squid giant axon. Mathematical models. *Biophys. J.* **3**:399.

HOYT, R. C. 1968. Sodium inactivation in nerve fibers. *Biophys. J.* **8**:1074.

KATZ, B. 1949. Les constantes électriques de la membrane du muscle. *Arch. Sci. physiol.* **3**:285.

KOPPENHÖFER, E. 1967. Die Wirkung von Tetraäthylammoniumchlorid auf die Membranströme Ranvierscher Schnürringe von *Xenopus laevis*. *Arch. gesamte Physiol. Menschen Tiere* (*Pfluegers*). **293**:34.

MOORE, J. W., T. NARAHASHI, and T. I. SHAW. 1967. An upper limit to the number of sodium channels in nerve membrane? *J. Physiol.* (*London*). **188**:99.

NAKAJIMA, S. 1966. Analysis of K inactivation and TEA action in the supramedullary cells of puffer. *J. Gen. Physiol.* **49**:629.

NAKAJIMA, S., S. IWASAKI, and K. OBATA. 1962. Delayed rectification and anomalous rectification in frog's skeletal muscle membrane. *J. Gen. Physiol.* **46**:97.

NAKAJIMA, S., and K. KUSANO. 1966. Behavior of delayed current under voltage clamp in the supramedullary neurons of puffer. *J. Gen. Physiol.* **49**:613.

NOBLE, D. 1962. A modification of the Hodgkin-Huxley equations applicable to Purkinje fiber action and pace-maker potentials. *J. Physiol.* (*London*). **160**:317.

NOBLE, D., and R. W. TSIEN. 1968. The kinetics and rectifier properties of the slow potassium current in cardiac Purkinje fibres. *J. Physiol.* (*London*). **195**:185.

SCHMIDT, H., and R. STÄMPFLI. 1966. Die Wirkung von Tetraäthylammoniumchlorid auf den einzelnen Ranvierschen Schnürring. *Arch. gesamte Physiol. Menschen Tiere* (*Pfluegers*). **287**:311.